Melanin-based electronics: From proton conductors to photovoltaics and beyond

Ehsan Vahidzadeh [†, a], Aarat P. Kalra [†, a, b] and Karthik Shankar [a]

[a] Department of Electrical and Computer Engineering, University of Alberta, 9107–116 St, Edmonton, Alberta T6G 2V4, Canada

[b] Department of Physics, University of Alberta, 11335 Saskatchewan Dr NW, Edmonton, Alberta T6G 2M9, Canada

†Authors who contributed equally to this work.

*Corresponding author: Karthik Shankar, kshankar@ualberta.ca

Abstract

The successful interfacing of electronics with biology is the next frontier for microelectronics and nanotechnology. Melanin, a naturally occurring conjugated polymer composed of different structural subunits, may be an ideal candidate for such interfacing. In the solid-state, the large broadband molar attenuation coefficient of melanin over the visible spectrum implicates potential applications as a semiconductor for light harvesting and light detection. Additionally, the conductance of melanin has been shown to increase with hydration, making this irregular polymer a hybrid electronic-protonic semiconductor. While the precise mechanism of charge transfer in melanin is not well understood, the hydration dependence of conductance has been tapped to utilise melanin-based devices in a variety of roles, such as humidity sensors and pH detectors. The applications of melanin active layers in OLEDs, OPVs, OFETs and batteries have also been explored. The viability of this polymer has also been validated inside biological systems, showing the potential for creating electronic devices that are biocompatible. This paper reviews the status of melanin towards achieving biocompatible electronics.

KEYWORDS: Optoelectronic Biomaterials; Bioelectronic Sensors; Eumelanin; Organic Electrochemical Transistors; Biophotovoltaics; Implantable Devices;

Table of Contents

1. Introduction

The past few decades have seen nanotechnology evolve at a rapid pace (Kurtz et al. 2017). As global warming and environmental degradation become realities with repercussions on local climates and public health, research into sustainable and biodegradable nanomaterials has become crucial (Bettinger and Bao 2010). Recently, effective integration with medicine has become a new frontier for progress. Naturally occurring macromolecules, being biodegradable and sustainable, are optimal candidates for future investigation. Their large-scale availability and pre-existing compatibility with biology make them attractive avenues for future research. A few such polymers

have been utilised as substrates for electronic devices. Silk, which is low-cost and readily available, was used as a substrate to create largely bio-resorbable devices where silicon was used as a nano-membrane (Kim et al. 2009). Silk fibroin pockets have been shown to reduce the degradation of transient electronic devices by reducing water contact (Brenckle et al. 2015). Commercial paper has also been used as a substrate for thin-film transistors (Eder et al. 2004; Kim et al. 2004). The utility of naturally occurring polymers is not limited exclusively to substrates since biologically relevant polymers have also been used as active layers in electronic devices. DNA (deoxyribonucleic acid), the double helical polymer in the nucleus, has been shown to have potential applications in nano-electronics, nanoscale robotics and computation (Steckl 2007; Taniguchi and Kawai 2006). In OLEDs, when DNA was complexed with cetyltrimethylammonium chloride (CTMA) surfactant to form an electron-blocking layer, it resulted in an improvement in efficiency by a factor of 10 and an improvement in brightness by a factor of 30 (Hagen et al. 2006). However, the mechanism of charge transport in DNA is unclear (Beratan et al. 1997; Endres et al. 2004) and could limit the large-scale production and optimisation of DNA based electronic devices. Furthermore, contamination with DNA may also be an issue (Bhalla et al. 2003). In this respect, the polymer chitosan is purported to have remarkable potential. Chitosan is derived from chitin, which makes up the exoskeleton in arthropods. Indeed, chitosan-based polysaccharide conductors were used to create artificial synapses on a paper substrate (Wu et al. 2014). A field-effect transistor was developed using maleic-chitosan nanofibers that could achieve modulation of protonic current (Zhong et al. 2011). However, the presence of free amino and hydroxyl groups makes chitosan hydrophilic; it swells when exposed to water. This makes it incompatible as a dielectric material in field-effect transistors wherein the semiconductor layer is

deposited from aqueous solutions (Singh et al. 2018). Chitosan thin films are also brittle, restricting potential use in biological conditions where flexibility is required (Rodríguez-Núñez et al. 2014).

Melanins, which are pigments found ubiquitously in the biosphere, have emerged in the past few years as a strong candidate for use in organic devices. OLEDs, OFETs, OPVs, OECTs and batteries have been fabricated using these polymers in the active layers of the aforementioned devices. Melanin is a cheap, natural, soft, biodegradable and biocompatible material with unique properties such as UV-Vis light absorption, mixed electronic-ionic conductivity and hydration state-dependent electrical conductivity. In addition to these remarkable properties, melanin can be manipulated to form really uniform and adherent thin films which is a prerequisite for applications in electronic devices. A timeline showing the progress of melanin related electronics is displayed in Fig. 1. An observation of the number of articles published with the "melanin" key word shows a trend indicative of the expanding research in this field (inset of Fig. 1). Within the animal kingdom, melanins are classified based on the presence of a group, into eumelanin (which imparts brown to black coloration) and phleomelanin (red to yellow coloration). This work will not distinguish between various types of melanin, nor the sources from which they were derived. Being inexpensive, naturally occurring and biocompatible, this material has a multitude of unique properties that lend themselves for utilisation in biosensing and organic electronic devices. Broadband electronic absorption and conduction through both electronic and ionic means are some hallmarks of melanin-based electronics and will be discussed in this work. We will then review the roles that melanins have been utilised in, for organic devices. After introducing the reader to conduction properties, we will provide an in-depth review of their versatility for use in several applications. For a more comprehensive review of other biomaterials and biopolymers with

potential applications to electronics, readers are referred to two excellent works (Feig et al. 2018; Irimia-Vladu et al. 2013).

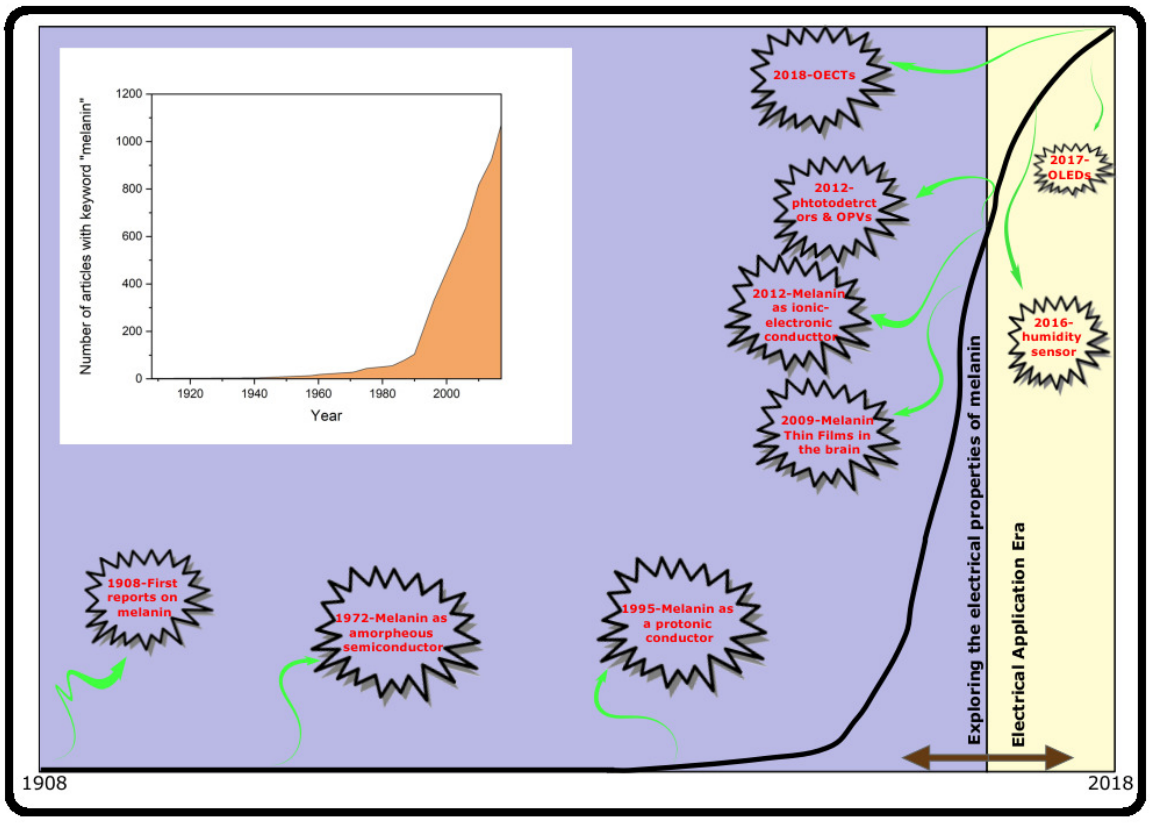

Fig. 1. A brief timeline of melanin-based electronics research. The black line represents the number of publication with the keyword "melanin" and key milestones in melanin-based electronics research.

2. Chemical Structure

Functionally, melanins play a role in determining the appearance of organisms. Over thousands of years, organisms have evolved to regulate melanin content in tissue to attenuate colour to precisely meet environmental demands. In insects, melanin in the outer layer of the exoskeleton can camouflage with the surroundings. In insects, melanin plays roles in coloration, wound healing and innate immunity (Bilandžija et al. 2017; Tapia et al. 2014; True 2003). In larger organisms such as birds, melanin regulates the vast diversity of feather colour, which can be used for a variety

of purposes, such as advertising, defense and concealment (Haase et al. 1992; Negro et al. 2018; Shiojiri et al. 1999). Among mammals and human beings, melanin content is directly related to skin and hair color, with a higher melanin content being associated with darker attributes (Jablonski and Chaplin 2000, 2010).

While the pigment itself was discovered more than a century ago, the structure of melanin has been hard to resolve. This is due to water insolubility over a broad pH range, irregular arrangement of constituent subunits and a lack of reliable methods to purify these constituents (Wakamatsu and Ito 2002). Melanin is primarily composed of DHI (5,6-dihydroxyindole) subunits linked at the 2, 3, 4 and 7 positions. The synthesis of melanin in vitro has been reviewed extensively in the literature (Prota and Misuraca 1997; Riesz et al. 2006; Solano 2014). Briefly, L-tyrosine is oxidized to L-dopa (L-3,4-dihydroxyiphenylalanine), which auto-oxidizes to form DHI and DHICA (5,6-dihydroxyindole-2-carboxylic acid). Both DHI and DHICA can oxidize further leading to the generation of oxidative pyrroles (pyrrole-2,3-dicarboxylic acid and pyrrole-2,3,5-tricarboxylic acid). Additionally, DHI and DHICA each exist in three redox states, resulting in irregularity in the polymeric structure. In addition to L-dopa, DHI, DHICA and their various redox states, the final melanin sample also contains their pyrroles, yielding a highly amorphous long-range structure (Fig. 2B). It is thus difficult to control the exact percentages of each of the monomers, because minor environmental factors during polymerization can lead to major structural changes in melanin. Fig. 2A is a schematic diagram of the structure of these monomers (Kaxiras et al. 2006; Meng and Kaxiras 2008). Studies also revealed that melanin was organized as stacked sheets with a vertical stacking distance of between 3.5 – 4 Å, implicating π-stacking (Dreyer et al. 2012; Kaxiras et al. 2006; Watt et al. 2009).

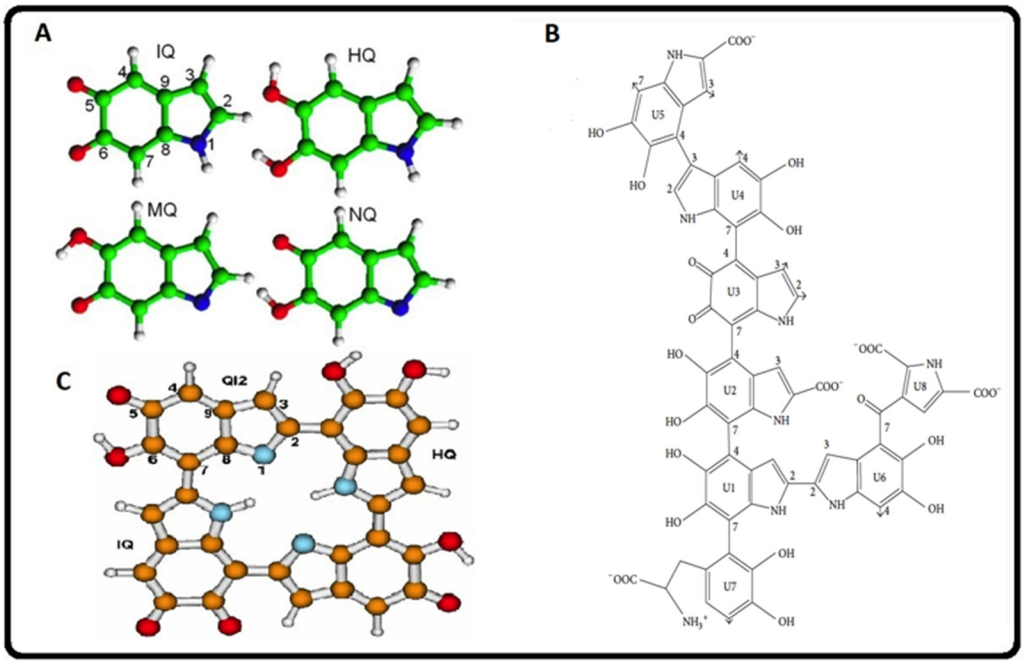

Fig. 2. The structure of melanin (A) Schematic of the main monomers comprising the melanin (green, C, red, O, blue, N, and white, H). Reprinted with permission from (Meng and Kaxiras 2008) (B) The two-dimensional structure of melanin is an irregular mixture of DHI (shown here in U1, U4 and U6), DHICA (U2 and U5), IQ (5,6 indolequinone, U3), L-dopa (U7) and carboxylated pyrroles (U8). Reprinted with permission from (Solano 2014); copyright (2014) Hindawi publishing corporation. (C) Proposed schematic for describing the structure of melanin as a tetramer (gold C, red O, blue N, and white H). Reprinted with permission from (Kaxiras et al. 2006);

3. Physicochemical properties

3.1 Optical properties

It is well established that melanins are photo-protective – they protect the skin against the harmful effects of ultraviolet (UV) and visible radiation (Brenner and Hearing 2008; Simon 2000). As a result, investigation of its optical properties has been the center of attention for several decades. It was shown that melanin is capable of dissipating 99 % of the absorbed UV and visible radiation through non-radiative means, making it an optimal photo-protector (Meredith and Riesz 2004).

Melanin also has a broadband, featureless absorption spectrum that extends across the visible and UV regions extending into the near-infrared (NIR), with the extinction coefficient decreasing exponentially and monotonically for longer wavelength photons (Fig. 3) (Riesz et al. 2006). Such an absorption spectrum is unusual for biological pigments, which usually display peaks at specific wavenumbers. The uniformly high, broadband absorption observed for melanins has been explained to arise from each of the various components in melanin absorbing different wavelengths, leading to net extinction over a broad range (Bolivar-Marinez et al. 1999; Powell et al. 2004; Riesz et al. 2006; Tran et al. 2006) (Fig. 3). While this 'chemical disorder model' can explain broadband absorption, the trend of an increasing absorption coefficient at high photon energies is not well understood. Recently, a report performing DFT (density functional theory) simulations of melanin showed that the absorption trend could be explained by accounting for the disorder in packing present among various vertical sheets of melanin (Chen et al. 2014).

A relation between particle-size and optical absorption has also been proposed. It has been shown that the optical spectrum of eumelanin displays a trend dependent on particle size, with a stronger extinction coefficient at longer wavelengths for higher molecular weight polymers (Simon 2000). This was hypothesized to arise due to either increased electron delocalization or increased optical scattering with higher particle sizes (Wolbarsht et al. 1981). The role of scattering was later refuted when it was found that scattering contributed to below 6 % of the total optical attenuation between 210 nm and 800 nm (Riesz et al. 2006). Kollias et al. also proposed that the absorption of melanin followed a linear trend in the entire visible region, and exhibited an exponential trend only in the 400-500 nm region (Kollias and Baqer 1987).

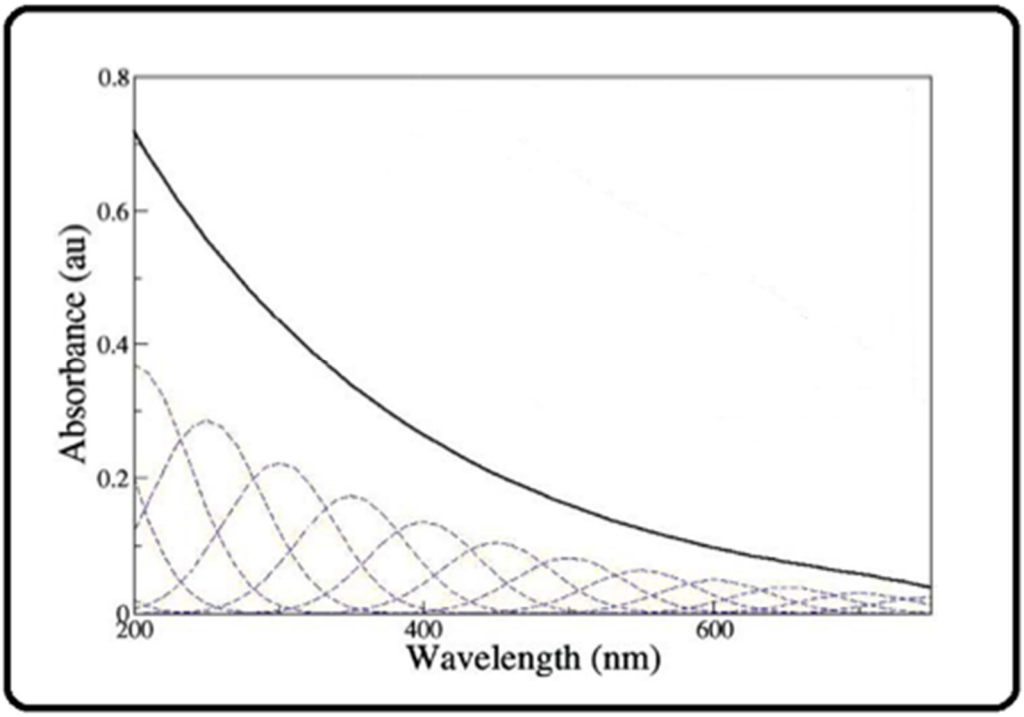

Fig. 3. The UV-visible absorbance spectrum of melanin. The broadband spectrum is explained as arising from a mixture of species present in the polymer, including L-Dopa, DHI, DHICA, their redox forms and their pyrroles. The graph depicts a spectrum with 15 species present (dashed Gaussians), which result in broadband absorption. Image adapted with permission from (Meredith et al. 2006).

It has been reported that melanin is a fluorescent material under both UV and visible light (Gallas and Eisner 1987) however, with an extremely weak emission signal (Huang et al. 2006; Meredith and Riesz 2004). The fluorescence spectrum of melanin depends on its concentration in solution and the excitation wavelength (Kozikowski et al. 1984; Meredith and Riesz 2004).

3.2 Paramagnetism

In 1954, it was discovered that naturally occurring melanin shows a distinct peak with a g-factor approaching 2 in electron spinning resonance (EPR), attributed to radicals trapped by this pigment (Commoner et al. 1954). Since then, it has become well known that naturally occurring melanin can exhibit paramagnetism, making EPR the leading characterization technique for understanding

the magnetic properties of this substance. To explain the origins of free radicals in melanin, Longuet-Higgins suggested that melanin behaves more like a one-dimensional semiconductor in which protons act as trap (Longuet-Higgins 1960). The equilibrium between concentrations of free radicals in a melanin solution can be described by the following equation (Chio et al. 1980):

$$QH_2 + Q \rightarrow 2SQ^{*} + 2H^{+} \quad 1$$

where QH_2, Q, and SQ^{*} represent the quinol units, quinone units, and free radicals respectively. Based on Le Chatelier's principle, in basic solutions, the reaction is shifted towards the products, while in acidic samples, it is shifted towards the reactants. Even though it has been reported that melanin's free radicals are stable even in harsh environments, number and type of free radicals in melanin has been reported to be dependent on several factors such as pH (Grady and Borg 1968), temperature (Chio et al. 1980), degree of hydration (Chio et al. 1980) and UV/Vis irradiation (Felix et al. 1979). In addition, it has been reported that the concentration of free radicals is strongly dependent on the concentration of reducing agents, oxidizing agents and metal ions in the environment. For example, paramagnetic metal ions such as Fe^{3+}, Cu^{2+} and Mn^{2+} decrease the free radical concentration and Zn^{2+} increases the concentration of free radicals in melanin solution (Buszman et al. 2005).

Even though the paramagnetic properties of melanin have been reported from the early 1950s, its origins are not yet fully understood. Experimental studies show that melanin has two paramagnetic centers. The first has a g-factor at approximately 2.003 and is widely observed in acidic media or melanin powder. This center has little dependence on temperature and pH and has been termed the carbon-centered radical (CCR). The second center has a g-factor of approximately 2.005 with a strong dependence on pH, and is called the semiquinone free radical (SFR) (Mostert et al. 2013).

Recently, the presence of these centers has been proven by Batagin et al. using a DFT approach (evaluations of g-factors and hyperfine interaction constants). Their theoretical calculations confirmed that there are at least two distinct paramagnetic centers in the melanin structure with different g-factors, which are the carbon centered radicals (CCR) and semiquinone free radicals (SFR) (Batagin-Neto et al. 2015).

3.3 Charge transport

The bioelectric potential of melanin was indicated in the early 1970s, when the semiconducting behavior of melanin was explained using the Mott-Davis amorphous semiconductor (MDAS) theory (McGinness et al. 1974; McGinness 1972; Powell and Rosenberg 1970). Due to extensive π-conjugation (as shown in Fig. 2B), electrons are delocalized across the polymer. However, melanin also has a high density of trap states originating in structural disorder, the different energy levels of the constituent sub-units and the presence of radical ions. Trapping induces localization of charge carriers due to which there exist mere pockets of mobile electrons in the polymer, which leads to a 'tailing' seen in the band gap structure (Fig. 4A). The effective 'optical gap' for melanin was calculated to be 3.4 eV (Crippa et al. 1978). Investigations showed that conduction in melanin was due to negatively charged carriers. Using DC measurements, Osak and co-workers also showed that while Ohm's law was followed at lower voltages, Child's law was followed at higher voltages (Osak et al. 1989).

Interestingly, the solid-state conductivity of melanin was seen to be a function of water content. The 'switching' observed by McGinness and co-workers occurred only when the sample was hydrated (McGinness et al. 1974). Thermally stimulated depolarization currents (TSDC) and 'non polarizing' electric field TSDC results showed that in addition to its' purported properties as

an amorphous semiconductor, water molecules trapped in the melanin tablet also contributed to its electrical behavior (Baraldi et al. 1979).

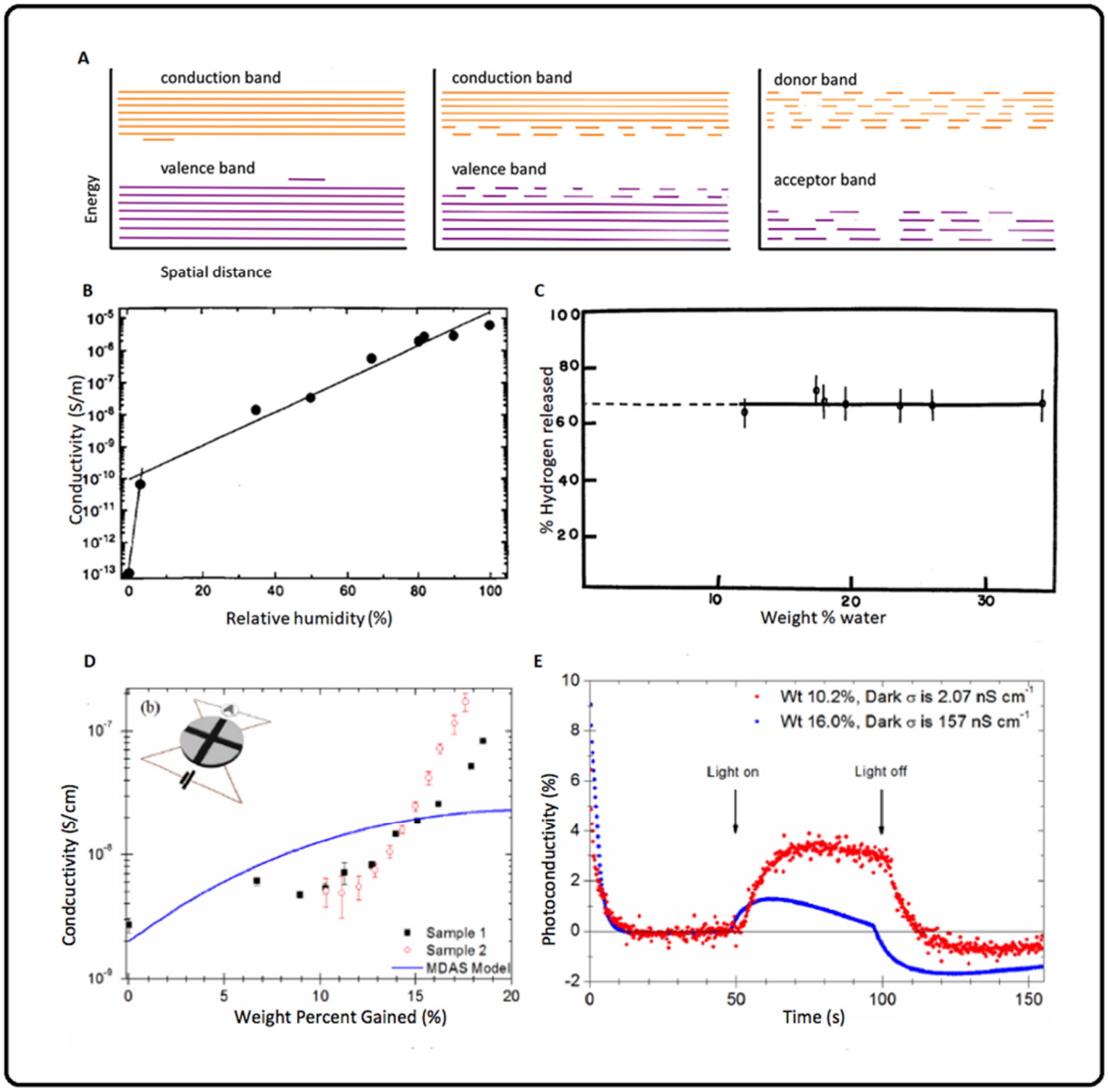

Fig. 4. Protonic charge transport in melanin. (A) Band diagram of a classical semiconductor (left), a semiconductor with short-range order (centre), and an amorphous semiconductor (right). The phenomenon of band 'tailing' seen here arises from the spatially localised electronic distribution present in the melanin polymer. Image inspired by (Lewis 1982) (B) Conductance depends inversely on humidity. Reprinted with permission from (Jastrzebska et al. 1996); copyright (1996) Taylor & Francis group (C) Electrolysis of a melanin sample shows the relative contribution of protons in the conductance. Reprinted with permission

from (Powell and Rosenberg 1970); copyright (1970) Springer (D) Reprinted with permission from (Wünsche et al. 2015); copyright (2015) American Chemical Society (E) The disparity between the observed conductivity and the MDAS-predicted conductivity shows the drawbacks of this theory. Reprinted with permission from (Bernardus Mostert et al. 2012); copyright (2012) American Institute of Physics.

The dependence of conductivity on humidity was found to be exponential (Fig. 4B) (Jastrzebska et al. 1996). However, when this trend was extended to 0 % humidity, it resulted in a conductivity value that was two orders of magnitude lower than the expected value. This is explained to arise from two types of water being present in melanin - one type is present on the surface and is easily removed by evaporation while the second type is present inside the melanin structure between stacked layers of the polymer and is not trivially removed. Hydrogen bonding takes place between water molecules and the carboxy-, hydroxyl- and amino groups of melanin. The results of Jastrzebska et al. (1996) also showed an inverse relationship between conductivity and temperature, which was explained as being a consequence of the decreasing humidity, which would lower the resistance. These conclusions were revisited more recently when, using transient current experiments with PdH_x electrodes at increasing humidity, it was shown that protonic charge transport was taking place (Wünsche et al. 2015). As expected, it was found that the current increased with increasing humidity and pellet dimensions. In addition to protonic charge transport, the authors pointed to contributions by redox processes between the various intermediates of the melanin subunits towards the net conductivity.

Hydration could also alter the energy band structure of melanin and attenuate the conductivity using a variety of mechanisms, which have been elegantly reviewed by Giacomantonio (Giacomantonio 2005). For instance, a chemical reaction in which water reacts with carboxy-, amino- and hydroxy- groups could take place, leading to the generation of H_3O^+ and COO^- ions, that could modify the energy band structure. Another mechanism is the adsorption of water

molecule on the outer surface of the melanin, which would serve to increase its' polarizability. A third mechanism considers the hydrogen bonded network that water forms around a polymer such as melanin. This network is purported to conduct protons via the Grotthus mechanism in the case of melanin. A combination of mechanisms may also be at play to induce the hydration dependence on the conductivity of melanin. Due to the dependence of conductance on hydration, protonic transport in addition to electronic transport was investigated and shown to occur, making it a 'mixed' type conductor. In a study on the types of conduction in various biological macromolecules, Powell and Rosenberg had shown that for melanin, 65 % of conductivity arose from protons, and this ratio did not change as the water percentage was increased from 12 % to 35 % as seen in Fig. 4C (Powell and Rosenberg 1970).

Recent work, however, shows that the MDAS theory may have limited applicability to melanin. To showcase this, Mostert and co-workers used an alternative van der Pauw (vdP) electrode geometry instead of the traditional sandwich-type geometry. The vdP geometry exposes samples to the environment effectively and yielded results with a significant deviation from the MDAS model. Based on these observations, the authors concluded that the previously used sandwich-type electrode geometry led to a systematic error in interpreting the charge transport characteristics of melanin. Again, when they measured the electrical conductivity of melanin as a function of its humidity, their results showed major discrepancies to the expectations from the MDAS theory (Fig. 4E) (Mostert et al. 2012). To explain this behavior, they used muon spin relaxation (μSR) spectroscopy, which showed that mobility of charge carriers is unaffected by hydration state of the melanin and that hydration added free radicals to the system, thus increasing the number of charge carriers. The authors concluded by rejecting the applicability of the MDAS theory to melanin and suggested that melanin should be considered as an electronic-ionic hybrid

conductor rather than an amorphous organic semiconductor (Bernardus Mostert et al. 2012; Mostert et al. 2012).

It may be noted that the MDAS theory accounted for dramatic changes in the electrical conductivity as the humidity changes (Mostert et al. 2012). However, as mentioned above, due to disparities observed between its predictions and experiments, a comprehensive model to describe the charge transport properties in melanin is yet to be developed. Creating such a framework for melanin has been difficult due to its hydration dependent electronic properties, and poor reproducibility arising from difficulties in fabricating smooth melanin films with good ohmic contacts (Bernardus Mostert et al. 2012).

4. Optoelectronic device applications

4.1 Photovoltaics

Owing to its broadband UV-Vis-NIR absorption, solution processability and low cost, the application of melanin in photovoltaic devices has attracted attention. The exploitation of eumelanin in photovoltaics is still in its embryonic stage and there are only a few reports on the use of this substance in the active layer of solar cells. Fig. 5A represents the preferred energy level alignment for an organic-inorganic hybrid heterojunction solar cell in which the lowest unoccupied molecular orbital (LUMO) of the electron donor (organic semiconductor) is located higher than the conduction band of the acceptor (inorganic semiconductor), while the donor highest occupied molecular orbital (HOMO) is located higher than the valence band edge of the acceptor (Antidormi et al. 2017) in order to achieve efficient separation of photogenerated carriers. In addition to the band alignment criterion which should be met to obtain high photovoltaic performance, the adhesion between the donor and acceptor layers is also of great importance as a necessary condition to achieve intimate electronic contact. To investigate the possible application of

eumelanin in a solar cell, Antidormi et al. (Antidormi et al. 2017) performed a comprehensive DFT study on the band alignment and adhesion properties of Si/eumelanin hybrids where silicon constituted the acceptor and eumelanin constituted the donor layer. Due to the complex nature of melanin, they considered the structure of the melanin to be tetrameric (composed of two indolequinone (IQ) and two quinoneimine (NQ) monomers) which was previously proposed to be the most stable model for eumelanin (Kaxiras et al. 2006). They proposed 5 different configurations (Fig. 5B) which these four monomers can link to each other and form the eumelanin structure. In addition, each of these models can have 4 different electronic configurations differing in the number and location of carbonyl terminations in the basic monomers (one =O group, two =O groups, four =O groups, and six =O groups). The adhesion studies calculations revealed that the =O terminated monomers affect the adhesion energies on a Si surface and that molecules with higher number of =O groups (model 1-d) exhibited stronger adhesion to the Si surface. Among the different configurations, molecules with an intrinsically planar structure (model1-d) exhibited stronger adhesion to the Si surface. In addition, the band alignment studies (Fig. 5C) revealed that among the different proposed models, only planar ones (model 1-d and 2) exhibited the proper band alignment. Antidormi et al. further proposed that there is a relationship between interaction of eumelanin with Si substrate and the desirable band line-up with eumelanin molecules with planar structure which tend to stick to the Si substrate strongly, exhibiting the most favorable band alignment for a hybrid solar cell.

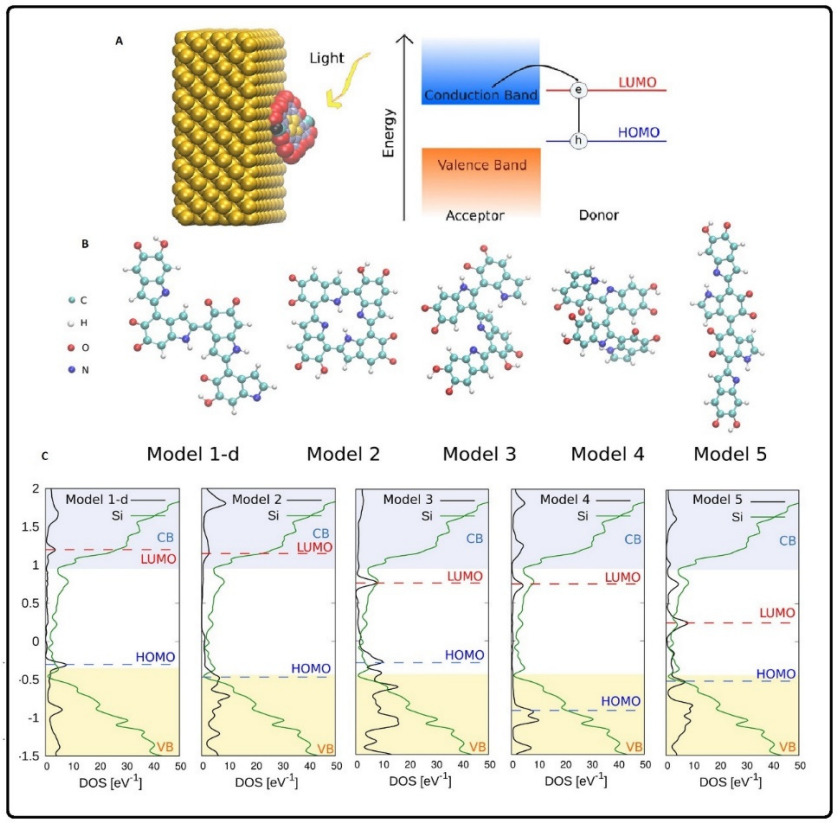

Fig. 5. (A) The band alignment suitable for heterojunction photovoltaic devices (B) Five tetramer models used for representing the structure of melanin. Reprinted with permission from (Antidormi et al. 2017); copyright (2017) American Chemical Society.

An experimental study on a bulk heterojunction made of porous silicon (p-Si) and eumelanin has been reported (Mula et al. 2012). Fig. 6A is a schematic illustration of the electrochemical etching setup which was used to synthesize the porous silicon samples in which the silicon served as the working electrode and a piece of platinum served as the counter electrode. The electrolyte used was HF and the substrate (working electrode) consisted of a 100-oriented, phosphorus doped n^+ Si wafer. Subsequently, the immobilization of the eumelanin on p-Si was achieved by treating the substrate with the appropriate solution/suspension of DHI or synthetic melanin; methanol, methanol/water, or a methanol/phosphate buffer pH 7.0 solutions were used as the liquid phase to deliver the eumelanin to the p-Si surface (Mula et al. 2012).

The heavily doped silicon substrate was the electron collection contact while the top gold electrode was the hole collection contact. Eumelanin and porous silicon formed a *p-n* bulk heterojunction with eumelanin as the donor and p-Si as the acceptor. The resulting photovoltaic device was illuminated by a tungsten halogen lamp at a maximum incident light intensity of 20 mW cm^{-2} (roughly 0.2 Sun). The device configuration is non-optimal since neither of the contact electrodes is transparent, due to which the device volume directly between the contacts can only receive scattered photons and much of the current collection is from the peripheral regions close to the edges of the gold electrode. Nevertheless, the eumelanin:p-Si bulk heterojunctions showed a highly promising performance that consisted of a maximum photovoltage of 0.15 V and a maximum photocurrent of 2.2 mA. Action spectrum testing constitutes a basic electrical characterization method for photovoltaic devices, and from these wavelength-dependent photocurrent measurements (Fig. 6C) for both bare p-Si and eumelanin:p-Si heterojunctions, it was seen that photocurrent monotonically increases when the wavelength decreases, which indicates that the absorption takes place in the whole available light spectrum. In addition, the eumelanin-impregnated p-Si samples showed a steep photocurrent increase in the lower energy part of the spectrum. This observation is in congruence with the fact that eumelanin exhibits higher optical absorption coefficients in higher wavelengths while p-Si has a weak absorption coefficient owing to the indirect bandgap of silicon. About 40 % of the total photocurrent is generated for impregnated samples by photons with wavelengths longer than 780 nm while for bare p-Si layers, the same wavelength range generated only about 15 % of the maximum photocurrent. The comparison between the maximum photocurrent achieved (I_{max}) is also proved helpful information, the I_{max} for the two p-Si samples were *ca.* 0.8 µA while this value for one of the impregnated samples was 1.1 µA. Although the reported performance was low, the obtained proof-of-concept

results clearly indicate that melanin/silicon based thin film heterojunctions have potential for use in hybrid photovoltaic devices and photodetectors.

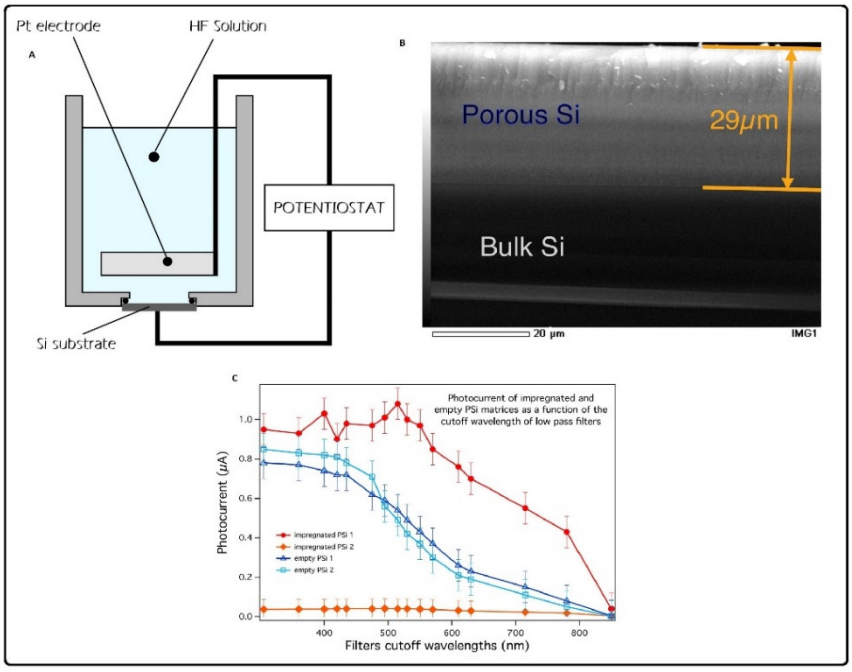

Fig. 6. (A) The anodization device for synthesis of porous silicon (p-Si) (B) SEM image of p-Si films (C) Results of photocurrent measurements reprinted from (Mula et al. 2012) under Creative Commons Attribution.

4.2 Light emitting diodes (LEDs)

The peculiar features of eumelanin such as water stability, adhesion properties and electronic-ionic conductivity, made it a possible candidate to improve the performance of organic electronic devices such as OLEDs. Migliaccio et al. attempted to improve the electrical conductivity and stability of PEDOT:PSS based OLEDs by blending PEDOT:PSS with eumelanin and making a stable film using these blends (Eu-PH films) (Migliaccio et al. 2017). The initial blend was prepared by spin-coating thin films from mixtures of DHI and PEDOT:PSS in water-isopropanol solutions containing a small amount of dimethylsulfoxide (DMSO). DHI present in the thin films was converted into eumelanin through ammonia-induced solid-state polymerization. The prepared blend made it possible to obtain transparent thin films which were stable in an aquatic environment

(the Eu-PH films exhibited good adhesion to the substrate even after 24 hours of immersion in water) (Migliaccio et al. 2017) and capable of improving upon the PEDOT:PSS electronic conductivity with the exotic eumelanin properties explained in Section 3.3. Fig. 7A represents the schematic diagram of the OLED device fabricated by Migliaccio et al. The hole transport layer (HTL) used in the OLED was a 40 nm-thick, thermally evaporated film of *N*,*N*′-di-1-naphthaleyl-*N*,*N*′-diphenyl-1,1′-biphenyl-4,4′-diamine (α-NPD) while thermally evaporated tris-8-hydroxyquinoline aluminum salt (Alq3) was used as the electron transport layer (ETL) and the emitting layer (EML, thickness 60 nm). Three different anode materials were investigated, namely PEDOT:PSS (PH 1000), ITO and EU-PH. Fig. 7B depicts the efficiency-voltage and efficiency-luminance curves of the devices with the three different anodes which clearly demonstrate that the efficiency of OLEDs with Eu-PH as a working anode is comparable to OLEDs that employ ITO as working anode with a lower turn-on voltage attributed to a smoother surface and better hole injection with Eu-PH. In addition, Fig. 7C and Fig. 7D also show the luminance and current density measured for the prepared OLEDs respectively, and the performance of the Eu–PH OLEDs was very close to the PH1000-based devices , which was remarkable considering that a blending weight ratio of 2:1 of DHI to PEDOT:PSS, was used to form the thin film anodes. The significance of these results is emphasized by the fact that Migliaccio et al. managed to fabricate and characterize ITO free OLEDs.

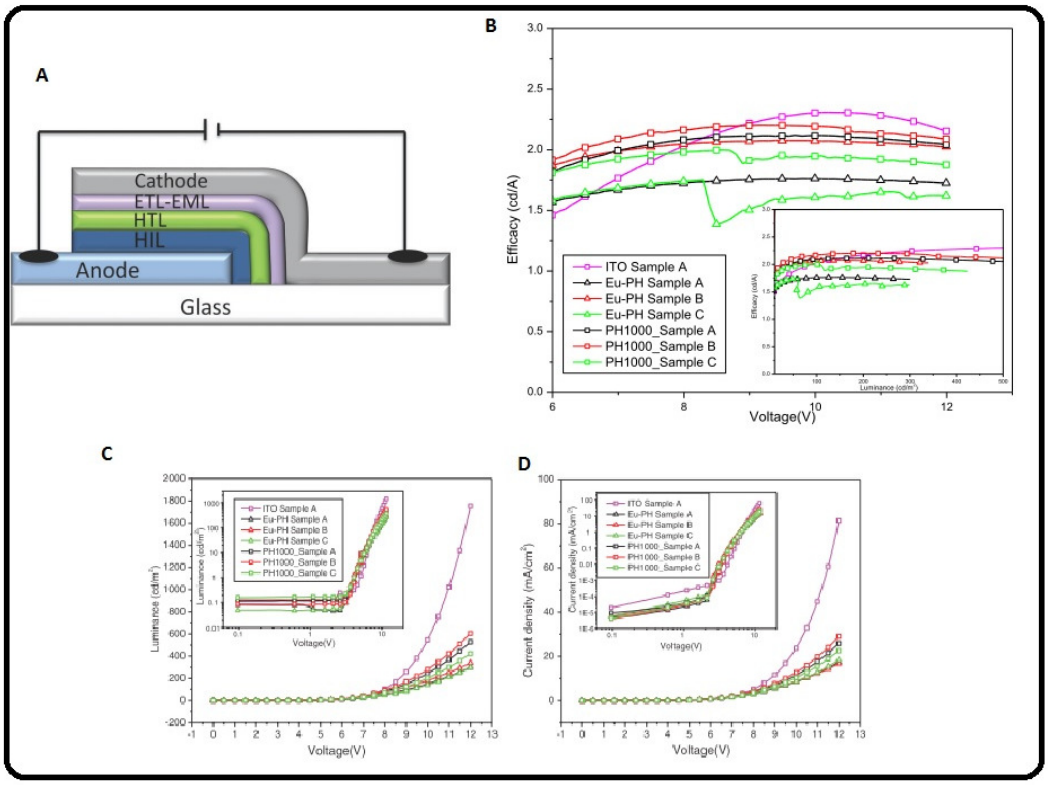

Fig. 7. (A) Schematic of the OLED device results of efficiency (B) Luminescence (C) and Current density (D) as a function of voltage reprinted with permission from (Migliaccio et al. 2017); copyright (2017) John Wiley and Sons.

4.3 Organic electrochemical transistors (OECTs)

Transduction between ionic signals and electronic signals is of increasing importance for bioelectronics since biological currents are ion-driven while currents in microelectronic devices are essentially electron-driven. Mixed conductors that can support both ionic and electronic currents are expected to play a prominent role in such ion to electron transducers. Melanin, as explained in Section 3.3, is such a mixed conductor. In this context, the most recent device application suggested for eumelanin is its application as an ion to electron transducer in an OECT (Sheliakina et al. 2018). The inset of Fig. 8A depicts the OECT device fabricated by Sheliakina et al. The Au source and drain electrodes were deposited first using vacuum thermal evaporation on a precleaned glass substrate followed by the solution deposition of a layer of PEDOT:PSS; next, a

layer of eumelanin was deposited using spin coating and in the final step, the gate electrode was deposited on top of the eumelanin active layer by a low temperature thermal evaporation technique. In this OECT, the melanin gate acted to modulate the conductance of the PEDOT:PSS channel. Since both the channel and gate materials are water-soluble, orthogonal solvent processing would normally be necessary to form patterned layers of each. A key processing innovation in the work of Sheliakina et al. that eliminated the need for orthogonal processing consisted of the use of a hexamethyldisilazane (HMDS) monolayer on top of the channel to prevent re-dissolution of the PEDOT:PSS during the deposition of melanin from aqueous solution. The typical transfer characteristics (I_D-V_{GS} plot for constant V_{DS}) and output characteristics (I_D-V_{DS} plots for various constant values of V_{GS}) of the fabricated transistors were measured in air and the results are shown in Fig. 8A and Fig. 8B respectively. Fig. 8B clearly shows that at a gate bias equal to zero, the fabricated OECT device was in ON state and applying a small positive voltage (1 V) turned the device OFF. Conduction in PEDOT:PSS is dominated by mobile holes that are compensated by immobile negative ions in the polymer backbone to preserve charge neutrality. The observed electrical behavior in the OECT occurs because the positive applied gate bias repels positive ions (protons) in the eumelanin layer and forces injection of these positive ions into the backbone of the PEDOT:PSS, de-doping it and reducing the hole concentration, which leads to a reduction of the source-drain current. Further investigation of the dependence of the sensitivity of the fabricated device to the moisture content was conducted by changing the partial pressure of the water vapor in the environment of the OECT, which required the use of a more flexible liquid metal eutectic Ga-In alloy gate contact instead of the gold electrode. From Fig. 8C, it can clearly be seen that in a dry environment (0 mbar water vapor partial pressure), the device does not show transistor behavior. Increasing the water vapor partial pressure (from 8 mbar to 18 mbar) led to a decrease

in the transistor turn off voltage since a continuous percolation network for proton conduction formed more easily in the melanin gate layer. The large hysteresis in the electrical characteristics of the devices (Fig. 8B and Fig. 8C) are typical of transistor action being dominated by the movement of ions rather than holes alone due to which this is an electrochemical field-effect transistor. These measurements clearly demonstrate that the hydration dependence of the electrical behavior of eumelanin is essential for the optimal operation of the OECT. An on/off ratio as high as 10^4 and a transconductance (g_m) as high as 175 µS was achieved.

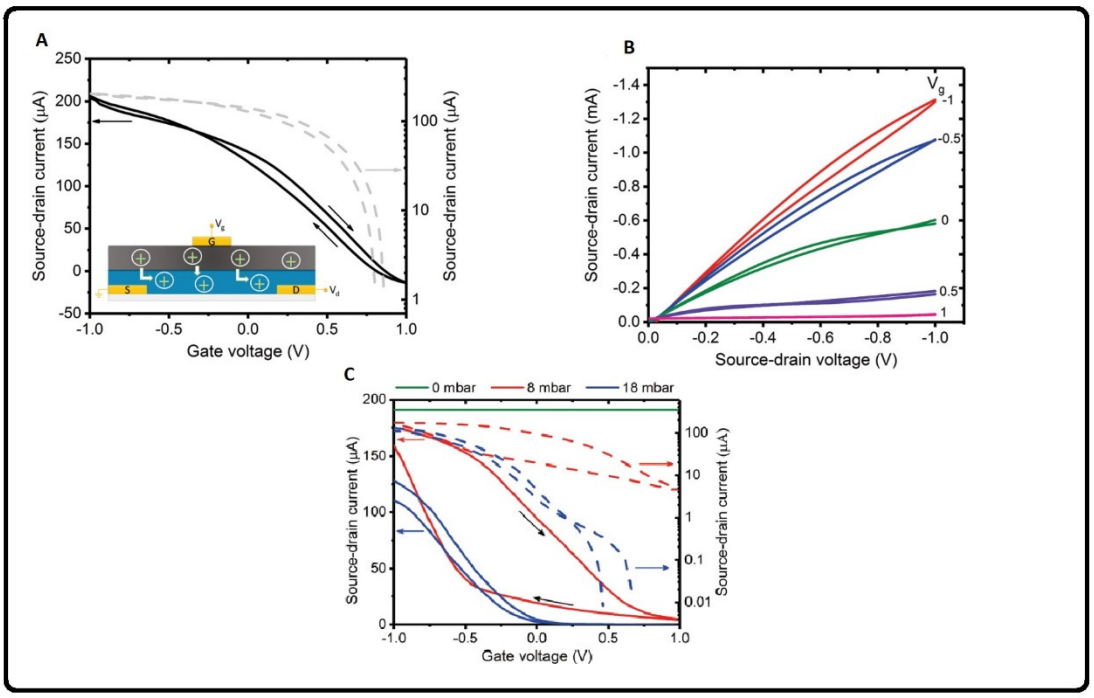

Fig. 8. (A) Measurements of the drain current as a function of gate voltage at a drain bias of 100 mV at a scan rate of 1 data point/s (B) Drain current as a function of drain bias and (C) Behavior of fabricated OECT under environments with different water vapor partial pressures. Reprinted with permission from (Sheliakina et al. 2018) under Creative Commons Attribution.

5. Applications as electronic sensing devices

Another interesting application of eumelanin is its application as a thin film humidity sensor (Wu and Hong 2016; Wu et al. 2015). Since the electrical conductivity of the eumelanin is strongly

dependent upon its hydration state (relative humidity of the environment), this parameter can be measured and used to quantify environmental relative humidity (RH). Recently Wu et al. successfully synthesized dopamine-melanin thin films that self-assembled at the air-solution interface. These self-standing films were mounted on a gold electrode and used as a humidity sensor (Wu et al. 2015). The schematic diagram of the setup for humidity sensing is shown in Fig. 9A and consists of electrical measurements across gold electrodes coated with dopamine-melanin. The *I-V* measurements for the prepared films under different values of the relative humidity were performed (Fig. 9B) and the resistance of the thin films was measured as a function of the relative humidity. In Fig. 9C, it is seen that the resistance of the prepared thin films decreased logarithmically as the relative humidity increased. The resistance of a 189 nm thick dopamine-melanin film at 0 % RH was found to be 430 times the resistance at 100 % RH (Wu et al. 2015). The pulse-stimuli characteristics of dopamine–melanin films, which were explored through a series of current responses to dynamic on/off switches at 100 % RH moisture are shown in Fig. 9D. From the on/off measurements, the prepared thin films exhibited a response time of roughly 5-7 s for moisture detection and 6-9 s for recovery.

Wu et al. once again used these dopamine-eumelanin thin films, this time mounted across interdigitated gold electrodes as a humidity sensor (Fig. 9E and Fig. 9F) for device applications (Wu and Hong 2016), and their results revealed that for both the humidity sensors fabricated by them, the logarithm of the resistance ($\log_{10}R$) increased linearly with decreasing relative humidity (Fig. 9G). Fig. 9D depicts the measured current when the flow of nitrogen was used to dynamically switch between wet and dry ambients. The fabricated sensor showed a much faster response time of 0.42-0.47 s and an ultrafast recovery time of 0.43-0.49 s.

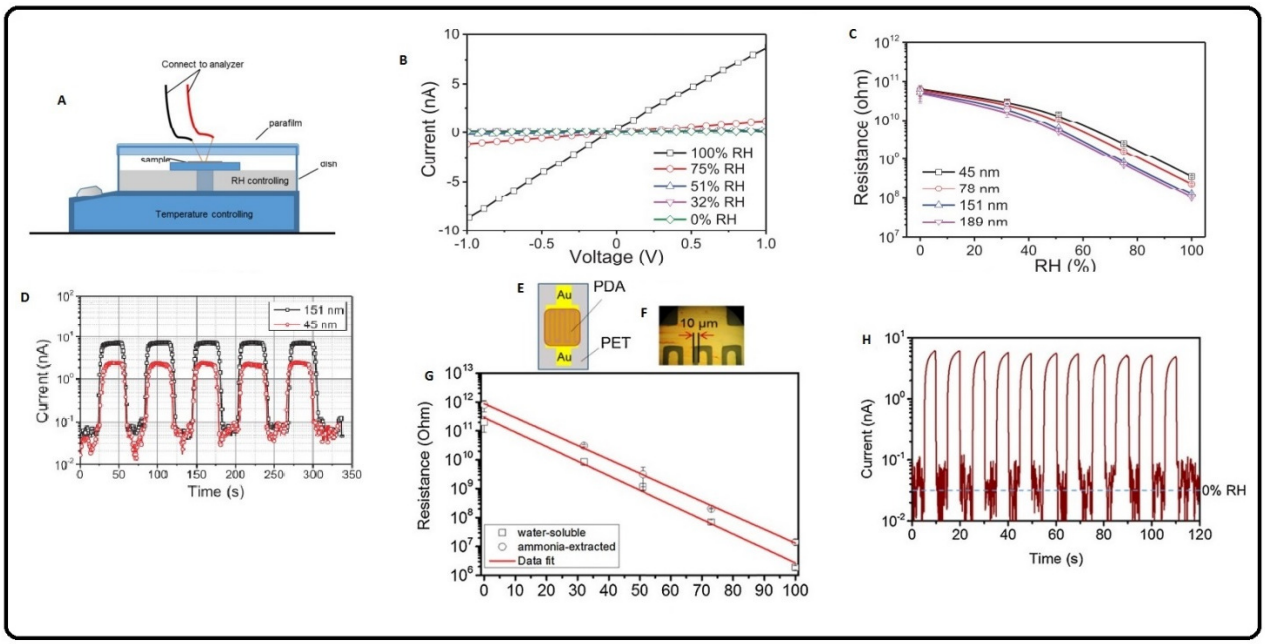

Fig. 9. The Schematic diagram of the static measurements for humidity sensor (A), I-V plots of the fabricated devices (B) and the corresponding calculated resistance as a function of relative humidity (C) and the results of dynamic sensitivity tests (D). Reprinted with permission from (Wu et al. 2015); copyright (2015) John Wiley and Sons The schematic (E) and optical microscopy pictures (E) of the fabricated device, the calculated resistance as a function of different relative humidity (G) and the results of dynamic sensitivity tests (H). Reprinted with permission from (Wu and Hong 2016); copyright (2016) Elsevier.

Extended gate field effect transistors (EGFETs) consist of an ion-sensitive layer on a conducting substrate directly connected to the gate of a commercial MOSFET, and constitute a more robust and durable configuration than ISFETs for measurements of pH and ion concentrations. Da Silva et al. fabricated an EGFET with melanin as the active ion sensing layer in their device (Piacenti da Silva et al. 2014). Solutions of melanin with three different concentrations were prepared (solution A, B and C) and then spin coated on the surface of ITO or gold deposited glass substrates. These devices were used as a EGFET in different pH solutions and typical measurements of source-drain current (I_{DS}) as a function of gate voltage and source-drain voltage were performed (Fig. 10A and Fig. 10B). The sensitivity of the fabricated device was determined by measuring the slope of the reference electrode vs pH curve at fixed I_{DS} (I_{DS} = 2 mA). The sensitivity

measurements revealed that the best device fabricated, showed a pH sensitivity of 48.9 mV/pH which is comparable by the other pH sensors reported in the literature. Da Silva et al. performed electrochemical impedance spectroscopy (EIS) on the melanin films, and used the EIS measurements in conjunction with EGFETs to determine the surface area and effective capacitance of the melanin films. Da Silva et al. were able to deduce that two types of interactions were responsible for the observed EGFET behavior of the melanin-based devices. One mechanism is based on the generation of a potential difference at the melanin-electrolyte interface due to the adsorption of ions in the Helmholtz plane and the second current-controlling mechanism involves the diffusion of protons from the electrolyte's Gouy-Chapman layer into the melanin film.

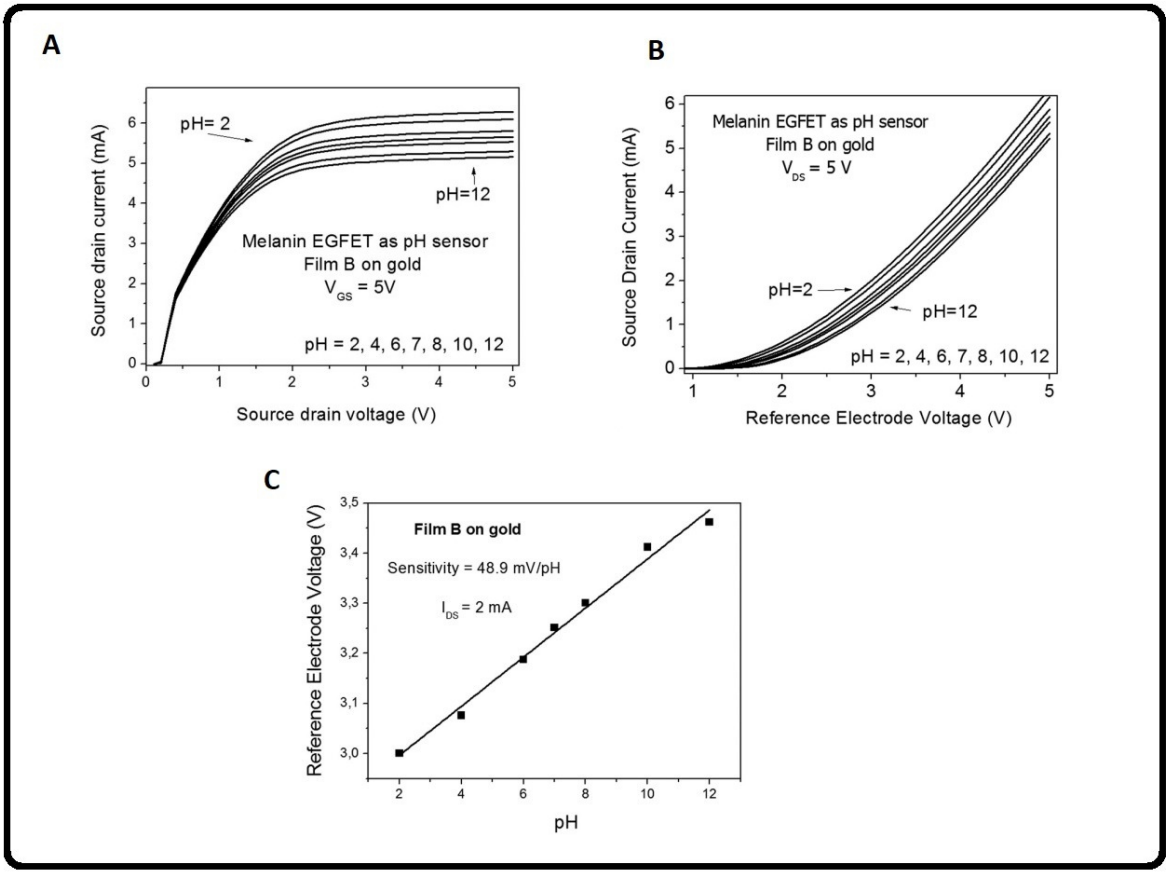

Fig. 1. Measurements of source-drain current as a function of source-drain voltage (A) Source-drain current as

a function of gate voltage (B) and the sensitivity measurement of the pH sensor (C) reprinted with permission from (Piacenti da Silva et al. 2014) under Creative Commons Attribution.

6. Applications in biocompatible electronics

To achieve biocompatibility, an implanted device must not, naturally, cause damage to biological tissue. Additionally, the non-toxic device must be flexible to mechanical deformation and stress, while being resistant to biochemical degradation. It must also continue performing in an unchanged manner and fulfill the role it was designed for. After this role has been completed, it must disintegrate without harming tissue if that is desired. Melanin-based devices have shown potential to fulfill such criteria, while performing roles as semiconductors within a thin film. It may be noted melanin and melanin-derived materials have already shown promise as biocompatible nanoparticles for biomedical applications (reviewed in (Solano 2017)).

Previously, electrical signals have been shown to inhibit the growth rate of cancer cells (Kirson et al. 2004), promote nerve cell regeneration (Schmidt et al. 1997), enhance formation of myofibers (Xia et al. 2000) and stimulate the proliferation of myoblasts (Pedrotty et al. 2005). To perform such a stimulation, a suitable conducting biocompatible platform is required. The biocompatible potential for melanin was hinted at, when both in vitro and in vivo studies showed that cells could attach and proliferate on melanin thin films (Bettinger et al. 2009). Bettinger and co-workers started out by drop-coating melanin dissolved in DMSO on SiO_2 substrates and testing the in vitro growth of Schwann cells on these thin films. It was seen that the Schwann cell proliferation was higher and longer-lasting on melanin thin films as opposed to collagen-coated or uncoated SiO_2 substrates (Fig. 11A and Fig. 11B). When the authors extended their study by implanting melanin in the sciatic nerve, to test in vivo biocompatibility, they found that the melanin thin film was stiff and fragmented due to mechanical stress from neighboring tissue (Fig. 11C).

Acute inflammation was also observed in proximity of the melanin implant. However, it may be noted that melanin degraded almost fully after eight weeks compared to the silicone control that did not degrade. This result highlighted the need to develop a process to make the films mechanically flexible.

To characterize biocompatibility, Piacenti-Silva and co-workers cultured Human gingival fibroblast cells on thin-films of melanin analogues that they fabricated (Piacenti-Silva et al. 2016). If the cells grew and were viable for an extended period, they hypothesized that it would be a step closer to achieving melanin-based biocompatibility. Two analogues of melanin were tested: The analogue D-Mel, which is soluble in DMSO (and hence presents itself as an advantage by not being soluble in NaOH), and W-mel, that was synthesized in water. The thin-film of D-Mel was fabricated in DMSO while that of W-Mel was fabricated in NH_4OH. Interestingly, it was seen that the cells had a higher viability when grown on the D-Mel thin-films for longer than 24-hour durations. The authors attributed the increased viability due to the presence of sulfonate groups that could potentially enhance biocompatibility. Such findings on the viability of cell growth on melanin thin-films have now set the stage for applications in biocompatible electronics.

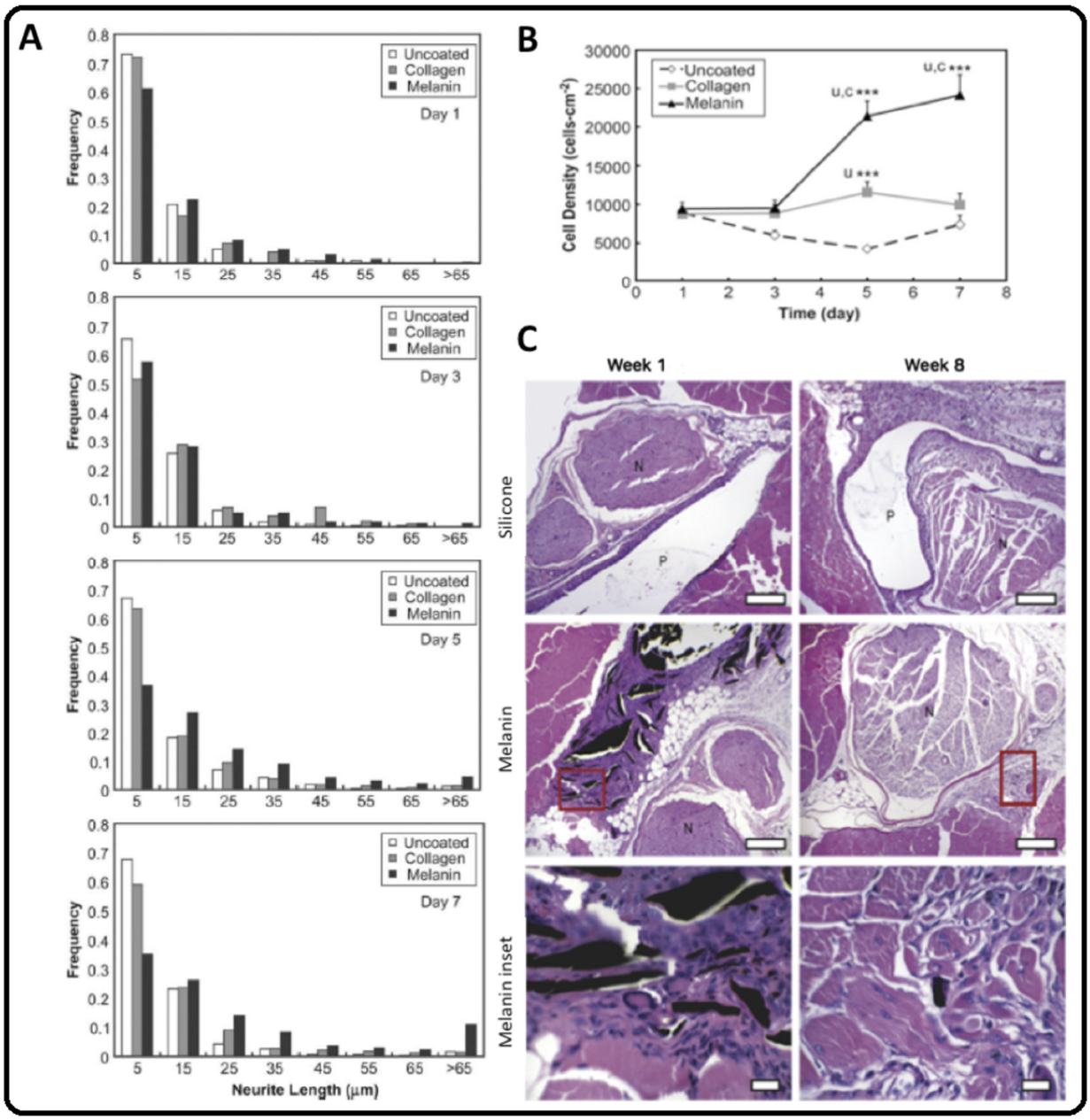

Fig. 2. The use of melanin thin-films in biological applications. (A) A display of the viability of Schwann cell growth on melanin coated glass, as opposed to Collagen or uncoated glass. (B) A graph showing that the cell density of cells grown on melanin thin-film is higher than that when Collagen is used. (C) Images showing the inflammation caused by melanin in mouse tissue. Reprinted with permission from (Bettinger et al. 2009); Copyright (2009) Elsevier.

7. Conclusions

Melanins are a family of amorphous polymers composed of L-dopa, DHI, DHICA, their redox forms and other intermediates. In addition to playing biological roles such as photoprotection and pigmentation, these polymers are interesting for optoelectronic device applications due to their irregular π-conjugated structure. In addition to extensive electronic delocalization because of conjugation, their conductance also varies with hydration implicating protonic charge transport. This work provides an overview of melanin-based electronics, not discriminating between eumelanin, phleomelanin or other forms of melanin. The uniqueness of melanin is several-fold. First, this semiconductor is naturally biocompatible, heightening its' potential in medical devices and implantable electronics. Although significant breakthroughs have been made possible through recent work (Bettinger et al. 2009; Kim et al. 2013; Piacenti da Silva et al. 2014; Piacenti-Silva et al. 2016), future work extending these ideas to fabricate devices that function in vivo and within human tissue present exciting avenues for research. Secondly, while most modern devices function on electronic transport, biological cells rely primarily on ionic transport and modulation of ion concentrations for signaling. Melanin exhibits mixed-type charge transport, making it an ideal interface to utilize electron-based devices in ion-based cellular environments. Outside physiology, with the advent of global warming and pollution, creation of biodegradable devices that can convert between electronic and ionic modes of conduction is increasingly relevant. Melanin is also soft and readily manipulated to form adhesive thin-films, an important requirement for organic electronic devices. Indeed, significant progress has started through fabrication of melanin-based devices to form OLEDs, pH sensors and humidity detectors, as reviewed in this work. Thirdly, unlike most semiconductors, melanin can be electronically excited using a broad spectral range of photons, improving flexibility to couple alongside a variety of materials, over a multitude of roles,

including OPVs, OLEDs and photoelectrochemical biosensors. While several melanin-based devices have already been fabricated, optimization of these devices to enhance performance is required. A low-cost method for mass production of such devices is also presently unclear. Additionally, while biocompatibility has been demonstrated to an extent in mouse models, implanting melanin-based devices in the human physiology is required in the future. While the present development of melanin-based biocompatible electronics is encouraging, further work to showing the reparative/medical action using melanin-based electronics remains to be performed. While furthering the development of environmentally sustainable nanotechnology, melanin can thus provide the essential link that bridges the gap between modern medicine and organic electronics.

Acknowledgements

All authors thank NSERC for financial support. AK and EV thank Mourad Benlamri and Saatviki Gupta for useful discussions.

Competing Interests

The authors have no competing interests.

References

Antidormi, A., Melis, C., Canadell, E., Colombo, L., 2017. Assessing the Performance of Eumelanin/Si Interface for Photovoltaic Applications. The Journal of Physical Chemistry C 121(21), 11576-11584.

Baraldi, P., Capelletti, R., Crippa, P., Romeo, N., 1979. Electrical characteristics and electret behavior of melanin. Journal of The Electrochemical Society 126(7), 1207-1212.

Batagin-Neto, A., Bronze-Uhle, E.S., de Oliveira Graeff, C.F., 2015. Electronic structure calculations of ESR parameters of melanin units. Physical Chemistry Chemical Physics 17(11), 7264-7274.

Beratan, D.N., Priyadarshy, S., Risser, S.M., 1997. DNA: insulator or wire? Chemistry & biology 4(1), 3-8.

Bernardus Mostert, A., Powell, B.J., Gentle, I.R., Meredith, P., 2012. On the origin of electrical conductivity in the bio-electronic material melanin. Applied Physics Letters 100(9), 093701.

Bettinger, C.J., Bao, Z., 2010. Biomaterials-based organic electronic devices. Polym. Int. 59(5), 563-567.

Bettinger, C.J., Bruggeman, J.P., Misra, A., Borenstein, J.T., Langer, R., 2009. Biocompatibility of biodegradable semiconducting melanin films for nerve tissue engineering. Biomaterials 30(17), 3050-3057.
Bhalla, V., Bajpai, R.P., Bharadwaj, L.M., 2003. DNA electronics: DNA and electronics seem to be two different things, but a series of events has highlighted the unusual ability of DNA to form electronic components. EMBO reports 4(5), 442-445.
Bilandžija, H., Laslo, M., Porter, M.L., Fong, D.W., 2017. Melanization in response to wounding is ancestral in arthropods and conserved in albino cave species. Scientific reports 7(1), 17148.
Bolivar-Marinez, L., Galvao, D., Caldas, M., 1999. Geometric and spectroscopic study of some molecules related to eumelanins. 1. Monomers. The Journal of Physical Chemistry B 103(15), 2993-3000.
Brenckle, M.A., Cheng, H., Hwang, S., Tao, H., Paquette, M., Kaplan, D.L., Rogers, J.A., Huang, Y., Omenetto, F.G., 2015. Modulated degradation of transient electronic devices through multilayer silk fibroin pockets. ACS applied materials & interfaces 7(36), 19870-19875.
Brenner, M., Hearing, V.J., 2008. The protective role of melanin against UV damage in human skin. Photochemistry and photobiology 84(3), 539-549.
Buszman, E., Pilawa, B., Zdybel, M., Wrześniok, D., Grzegorczyk, A., Wilczok, T., 2005. EPR examination of Zn2+ and Cu2+ effect on free radicals in DOPA–melanin–netilmicin complexes. Chemical Physics Letters 403(1-3), 22-28.
Chen, C.-T., Chuang, C., Cao, J., Ball, V., Ruch, D., Buehler, M.J., 2014. Excitonic effects from geometric order and disorder explain broadband optical absorption in eumelanin. Nature communications 5, 3859.
Chio, S.-S., Hyde, J.S., Sealy, R.C., 1980. Temperature-dependent paramagnetism in melanin polymers. Archives of biochemistry and biophysics 199(1), 133-139.
Commoner, B., Townsend, J., Pake, G.E., 1954. Free radicals in biological materials. Nature 174(4432), 689.
Crippa, P., Cristofoletti, V.t., Romeo, N., 1978. A band model for melanin deduced from optical absorption and photoconductivity experiments. Biochimica et Biophysica Acta (BBA)-General Subjects 538(1), 164-170.
Dreyer, D.R., Miller, D.J., Freeman, B.D., Paul, D.R., Bielawski, C.W., 2012. Elucidating the structure of poly (dopamine). Langmuir 28(15), 6428-6435.
Eder, F., Klauk, H., Halik, M., Zschieschang, U., Schmid, G., Dehm, C., 2004. Organic electronics on paper. Applied Physics Letters 84(14), 2673-2675.
Endres, R.G., Cox, D.L., Singh, R.R., 2004. Colloquium: The quest for high-conductance DNA. Reviews of Modern Physics 76(1), 195.
Feig, V.R., Tran, H., Bao, Z., 2018. Biodegradable Polymeric Materials in Degradable Electronic Devices. ACS Central Science.
Felix, C., Hyde, J., Sealy, R., 1979. Photoreactions of melanin: a new transient species and evidence for triplet state involvement. Biochemical and biophysical research communications 88(2), 456-461.
Gallas, J.M., Eisner, M., 1987. FLUORESCENCE OF MELANIN-DEPENDENCE UPON EXCITATION WAVELENGTH AND CONCENTRATION. Photochemistry and photobiology 45(5), 595-600.
Giacomantonio, C., 2005. Charge transport in melanin, a disordered bio-organic conductor. University of Queensland.
Grady, F.J., Borg, D.C., 1968. Electron paramagnetic resonance studies on melanins. I. The effect of pH on spectra at Q band. J. Am. Chem. Soc. 90(11), 2949-2952.
Haase, E., Ito, S., Sell, A., Wakamatsu, K., 1992. Melanin concentrations in feathers from wild and domestic pigeons. Journal of Heredity 83(1), 64-67.
Hagen, J.A., Li, W., Steckl, A., Grote, J., 2006. Enhanced emission efficiency in organic light-emitting diodes using deoxyribonucleic acid complex as an electron blocking layer. Applied Physics Letters 88(17), 171109.

Huang, Z., Zeng, H., Hamzavi, I., Alajlan, A., Tan, E., McLean, D.I., Lui, H., 2006. Cutaneous melanin exhibiting fluorescence emission under near-infrared light excitation. Journal of biomedical optics 11(3), 034010.
Irimia-Vladu, M., Głowacki, E.D., Sariciftci, N.S., Bauer, S., 2013. Natural Materials for Organic Electronics. Small Organic Molecules on Surfaces, pp. 295-318. Springer.
Jablonski, N.G., Chaplin, G., 2000. The evolution of human skin coloration. Journal of human evolution 39(1), 57-106.
Jablonski, N.G., Chaplin, G., 2010. Human skin pigmentation as an adaptation to UV radiation. Proceedings of the National Academy of Sciences 107(Supplement 2), 8962-8968.
Jastrzebska, M.M., Isotalo, H., Paloheimo, J., Stubb, H., 1996. Electrical conductivity of synthetic DOPA-melanin polymer for different hydration states and temperatures. Journal of Biomaterials Science, Polymer Edition 7(7), 577-586.
Kaxiras, E., Tsolakidis, A., Zonios, G., Meng, S., 2006. Structural model of eumelanin. Physical review letters 97(21), 218102.
Kim, D.-H., Kim, Y.-S., Amsden, J., Panilaitis, B., Kaplan, D.L., Omenetto, F.G., Zakin, M.R., Rogers, J.A., 2009. Silicon electronics on silk as a path to bioresorbable, implantable devices. Applied physics letters 95(13), 133701.
Kim, Y.-H., Moon, D.-G., Han, J.-I., 2004. Organic TFT array on a paper substrate. IEEE electron device letters 25(10), 702-704.
Kim, Y.J., Wu, W., Chun, S.-E., Whitacre, J.F., Bettinger, C.J., 2013. Biologically derived melanin electrodes in aqueous sodium-ion energy storage devices. Proceedings of the National Academy of Sciences 110(52), 20912-20917.
Kirson, E.D., Gurvich, Z., Schneiderman, R., Dekel, E., Itzhaki, A., Wasserman, Y., Schatzberger, R., Palti, Y., 2004. Disruption of cancer cell replication by alternating electric fields. Cancer research 64(9), 3288-3295.
Kollias, N., Baqer, A.H., 1987. Absorption mechanisms of human melanin in the visible, 400–720 nm. Journal of investigative dermatology 89(4), 384-388.
Kozikowski, S., Wolfram, L., Alfano, R., 1984. Fluorescence spectroscopy of eumelanins. IEEE journal of quantum electronics 20(12), 1379-1382.
Kurtz, S., Haegel, N., Sinton, R., Margolis, R., 2017. A new era for solar. Nature Photonics 11(1), 3.
Longuet-Higgins, H., 1960. On the origin of the free radical property of melanins. Archives of biochemistry and biophysics 86(2), 231-232.
McGinness, J., Corry, P., Proctor, P., 1974. Amorphous semiconductor switching in melanins. Science 183(4127), 853-855.
McGinness, J.E., 1972. Mobility gaps: a mechanism for band gaps in melanins. Science 177(4052), 896-897.
Meng, S., Kaxiras, E., 2008. Theoretical models of eumelanin protomolecules and their optical properties. Biophysical journal 94(6), 2095-2105.
Meredith, P., Powell, B.J., Riesz, J., Nighswander-Rempel, S.P., Pederson, M.R., Moore, E.G., 2006. Towards structure–property–function relationships for eumelanin. Soft Matter 2(1), 37-44.
Meredith, P., Riesz, J., 2004. Radiative relaxation quantum yields for synthetic eumelanin. Photochemistry and photobiology 79(2), 211-216.
Migliaccio, L., Aprano, S., Iannuzzi, L., Maglione, M.G., Tassini, P., Minarini, C., Manini, P., Pezzella, A., 2017. Eumelanin–PEDOT: PSS Complementing En Route to Mammalian-Pigment-Based Electrodes: Design and Fabrication of an ITO-Free Organic Light-Emitting Device. Advanced Electronic Materials 3(5).
Mostert, A.B., Hanson, G.R., Sarna, T., Gentle, I.R., Powell, B.J., Meredith, P., 2013. Hydration-controlled X-band EPR spectroscopy: A tool for unravelling the complexities of the solid-state free radical in eumelanin. The Journal of Physical Chemistry B 117(17), 4965-4972.

Mostert, A.B., Powell, B.J., Pratt, F.L., Hanson, G.R., Sarna, T., Gentle, I.R., Meredith, P., 2012. Role of semiconductivity and ion transport in the electrical conduction of melanin. Proceedings of the National Academy of Sciences 109(23), 8943-8947.
Mula, G., Manca, L., Setzu, S., Pezzella, A., 2012. Photovoltaic properties of PSi impregnated with eumelanin. Nanoscale research letters 7(1), 377.
Negro, J.J., Finlayson, C., Galván, I., 2018. Melanins in Fossil Animals: Is It Possible to Infer Life History Traits from the Coloration of Extinct Species? International journal of molecular sciences 19(2), 230.
Osak, W., Tkacz, K., Czternastek, H., SłAwiński, J., 1989. I–V characteristics and electrical conductivity of synthetic melanin. Biopolymers 28(11), 1885-1890.
Pedrotty, D.M., Koh, J., Davis, B.H., Taylor, D.A., Wolf, P., Niklason, L.E., 2005. Engineering skeletal myoblasts: roles of three-dimensional culture and electrical stimulation. American Journal of Physiology-Heart and Circulatory Physiology 288(4), H1620-H1626.
Piacenti da Silva, M., Fernandes, J.C., de Figueiredo, N.B., Congiu, M., Mulato, M., de Oliveira Graeff, C.F., 2014. Melanin as an active layer in biosensors. Aip Advances 4(3), 037120.
Piacenti-Silva, M., Matos, A.A., Paulin, J.V., Alavarce, R.A.d.S., de Oliveira, R.C., Graeff, C.F., 2016. Biocompatibility investigations of synthetic melanin and melanin analogue for application in bioelectronics. Polym. Int. 65(11), 1347-1354.
Powell, B., Baruah, T., Bernstein, N., Brake, K., McKenzie, R.H., Meredith, P., Pederson, M., 2004. A first-principles density-functional calculation of the electronic and vibrational structure of the key melanin monomers. The Journal of chemical physics 120(18), 8608-8615.
Powell, M.R., Rosenberg, B., 1970. The nature of the charge carriers in solvated biomacromolecules. Journal of bioenergetics 1(6), 493-509.
Prota, G., Misuraca, G., 1997. Melanins and related metabolites in skin photoprotection. Skin Cancer and UV Radiation, pp. 148-157. Springer.
Riesz, J., Gilmore, J., Meredith, P., 2006. Quantitative scattering of melanin solutions. Biophysical journal 90(11), 4137-4144.
Rodríguez-Núñez, J.R., Madera-Santana, T.J., Sánchez-Machado, D.I., López-Cervantes, J., Valdez, H.S., 2014. Chitosan/hydrophilic plasticizer-based films: preparation, physicochemical and antimicrobial properties. Journal of Polymers and the Environment 22(1), 41-51.
Schmidt, C.E., Shastri, V.R., Vacanti, J.P., Langer, R., 1997. Stimulation of neurite outgrowth using an electrically conducting polymer. Proceedings of the National Academy of Sciences 94(17), 8948-8953.
Sheliakina, M., Mostert, A., Meredith, P., 2018. An all-solid-state biocompatible ion-to-electron transducer for bioelectronics. Materials Horizons.
Shiojiri, N., Niwa, T., Wakamatsu, K., Ito, S., Nakamura, A., 1999. Chemical analysis of melanin pigments in feather germs of Japanese Quail Bh (black at hatch) mutants. Pigment Cell & Melanoma Research 12(4), 259-265.
Simon, J.D., 2000. Spectroscopic and dynamic studies of the epidermal chromophores trans-urocanic acid and eumelanin. Accounts of chemical research 33(5), 307-313.
Singh, R., Lin, Y.T., Ko, F.H., 2018. Aqueous Solution-Processable, Flexible Thin-Film Transistors Based on Crosslinked Chitosan Dielectric Thin Films. Macromolecular Materials and Engineering.
Solano, F., 2014. Melanins: skin pigments and much more—types, structural models, biological functions, and formation routes. New Journal of Science 2014.
Solano, F., 2017. Melanin and melanin-related polymers as materials with biomedical and biotechnological applications—cuttlefish ink and mussel foot proteins as inspired biomolecules. International journal of molecular sciences 18(7), 1561.
Steckl, A.J., 2007. DNA–a new material for photonics? Nature Photonics 1(1), 3.
Taniguchi, M., Kawai, T., 2006. DNA electronics. Physica E: Low-dimensional Systems and Nanostructures 33(1), 1-12.

Tapia, C.V., Falconer, M., Tempio, F., Falcón, F., López, M., Fuentes, M., Alburquenque, C., Amaro, J., Bucarey, S.A., Nardo, A.D., 2014. Melanocytes and melanin represent a first line of innate immunity against Candida albicans. Medical mycology 52(5), 445-454.
Tran, M.L., Powell, B.J., Meredith, P., 2006. Chemical and structural disorder in eumelanins: a possible explanation for broadband absorbance. Biophysical journal 90(3), 743-752.
True, J.R., 2003. Insect melanism: the molecules matter. Trends in ecology & evolution 18(12), 640-647.
Wakamatsu, K., Ito, S., 2002. Advanced chemical methods in melanin determination. Pigment Cell & Melanoma Research 15(3), 174-183.
Watt, A.A., Bothma, J.P., Meredith, P., 2009. The supramolecular structure of melanin. Soft Matter 5(19), 3754-3760.
Wolbarsht, M., Walsh, A., George, G., 1981. Melanin, a unique biological absorber. Applied Optics 20(13), 2184-2186.
Wu, G., Zhang, J., Wan, X., Yang, Y., Jiang, S., 2014. Chitosan-based biopolysaccharide proton conductors for synaptic transistors on paper substrates. Journal of Materials Chemistry C 2(31), 6249-6255.
Wu, T.-F., Hong, J.-D., 2016. Synthesis of water-soluble dopamine–melanin for ultrasensitive and ultrafast humidity sensor. Sensors and Actuators B: Chemical 224, 178-184.
Wu, T.F., Wee, B.H., Hong, J.D., 2015. An Ultrasensitive and Fast Moisture Sensor Based on Self-Assembled Dopamine–Melanin Thin Films. Advanced Materials Interfaces 2(15).
Wünsche, J., Deng, Y., Kumar, P., Di Mauro, E., Josberger, E., Sayago, J., Pezzella, A., Soavi, F., Cicoira, F., Rolandi, M., Santato, C., 2015. Protonic and Electronic Transport in Hydrated Thin Films of the Pigment Eumelanin. Chemistry of Materials 27(2), 436-442.
Xia, Y., McMillin, J.B., Lewis, A., Moore, M., Zhu, W.G., Williams, R.S., Kellems, R.E., 2000. Electrical stimulation of neonatal cardiac myocytes activates the NFAT3 and GATA4 pathways and up-regulates the adenylosuccinate synthetase 1 gene. Journal of Biological Chemistry 275(3), 1855-1863.
Zhong, C., Deng, Y., Roudsari, A.F., Kapetanovic, A., Anantram, M., Rolandi, M., 2011. A polysaccharide bioprotonic field-effect transistor. Nature communications 2, 476.